arXiv:1403.7475v1 [cond-mat.mes-hall] 28 Mar 2014

Gate-modulated thermopower of disordered nanowires: II. Variable-Range Hopping Regime

Riccardo Bosisio, Cosimo Gorini, Geneviève Fleury and Jean-Louis Pichard‡

Service de Physique de l'État Condensé (CNRS URA 2464), IRAMIS/SPEC, CEA Saclay, 91191 Gif-sur-Yvette, France

Abstract. We study the thermopower of a disordered nanowire in the field effect transistor device configuration. After a first paper devoted to the elastic coherent regime, we consider here the inelastic activated regime taking place at higher temperatures. We consider the case where charge transport is thermally assisted by phonons (Mott Variable Range Hopping regime). For this purpose, we use the Miller-Abrahams random resistor network model as recently adapted by Jiang *et al.* for thermoelectric transport. This approach previously used to study the bulk of the nanowire impurity band is extended for studying its edges. In this limit, we show that the typical thermopower becomes very large and exhibits a non-trivial behavior as a function of the temperature. A percolation theory of Zvyagin extended to disordered nanowires allows us to account for the main observed edge behaviors of the thermopower.

PACS numbers: 72.20.Ee 72.20.Pa 84.60.Rb 73.23.-b 73.63.Nm

‡ Corresponding author: jean-louis.pichard@cea.fr

1. Introduction

The conversion of temperature to voltage differences or its inverse, enabling respectively waste heat recovery or cooling, is the purpose of thermoelectric devices. In linear response the latter's efficiency is measured via the dimensionless figure of merit $ZT = S^2GT/\Xi$, with T the temperature, S the Seebeck coefficient or thermopower and G, Ξ respectively the electrical and thermal conductances. The stronger the particle-hole *asymmetry* in a system, the higher S is. An ideal thermoelectric device should then exploit to the maximum such asymmetry, while at the same time ensuring a poor thermal and a good electrical conductance [1]. Whereas the former requirement is necessary to increase efficiency, the latter is needed if enough electric (cooling) power is to be extracted from a heat engine (Peltier refrigerator). From this perspective, semiconductor nanowires appear as very promising central building blocks of flexible, efficient and environmentally friendly thermoelectric converters [2, 3, 4, 5, 6, 7, 8]. Whereas their electronic properties can be easily tuned by gates [5, 8], the phononic contribution to thermal transport Ξ_{ph} is suppressed due to the reduced dimensionality [3, 4], and a good power output could be achieved by stacking them in parallel [9, 3, 6]. Furthermore Si-based devices, already under intense investigation [10, 11, 12, 9, 13, 14, 3, 15, 4, 6], exploit an abundant and non-polluting resource.

Most existing works concentrate either on highly doped samples [10, 12, 9, 3, 7, 6] or on the thermal conductivity of undoped wires [11, 14, 16, 15, 4]. On the other hand recent studies by Jiang *et al.* [17, 18] have rekindled the interest for systems in which electronic transport takes place via phonon-assisted hopping between localized states, of which disordered nanowires with low carrier density are a paradigmatic realization. In this work we extend the approach reviewed in Refs. [17, 18] in order to investigate band-edge hopping transport. Two simple physical mechanisms have in this regime a synergy which is ideal for thermoelectric conversion [19, 20]: (i) a strongly broken particle-hole symmetry due to the Fermi level lying close to the band edge; (ii) a wide energy window around the Fermi level made available for transport by the phonons. In other words, the phonons lend the carriers the energy necessary for them to hop through the system, but of the latter only one species, either electrons or holes, has available states and thus actually propagates.

The general setup we have in mind is a disordered semiconductor nanowire connected to two metallic leads, the wire being either suspended/surrounded by void [12, 9, 7, 6], deposited on a substrate or embedded in a matrix [3, 21, 22] – the substrate or the matrix being electrically and thermally insulating. The nanowire itself could be (i) lightly doped, with electrons localized around distant impurity states, or (ii) highly doped but strongly depleted, or (iii) made of an amorphous semiconductor. The abstraction of such a system will be that of a disordered 1D chain connected to two electronic reservoirs and to a phonon bath, which could in principle be an independent third terminal [18], and coupled to a gate used to modulate its carrier density [23, 5]. Depending on the particular realization the phonon bath would represent the wire, substrate or matrix phonons, whereas each chain site would correspond to electronic states localized by disorder or bound to impurity sites. Notice however that a variety of quasi-1D and quasi-metallic systems could be practical realizations of such a minimal model [24, 25, 26].

In this work we are primarily interested in the thermopower S of a single nanowire, as studied e.g. in a very recent experiment [5]. The issue of the efficiency and power output of a nanowire array will be dealt with elsewhere. We will start in Sec. 2 by introducing model and methods employed, moving on to discuss the nanowire electrical conductance in Sec. 3 and its thermopower in Sec. 4, before concluding in Sec. 5. Various technical details, skimmed over in the main body for ease of reading, are gathered in the appendices.

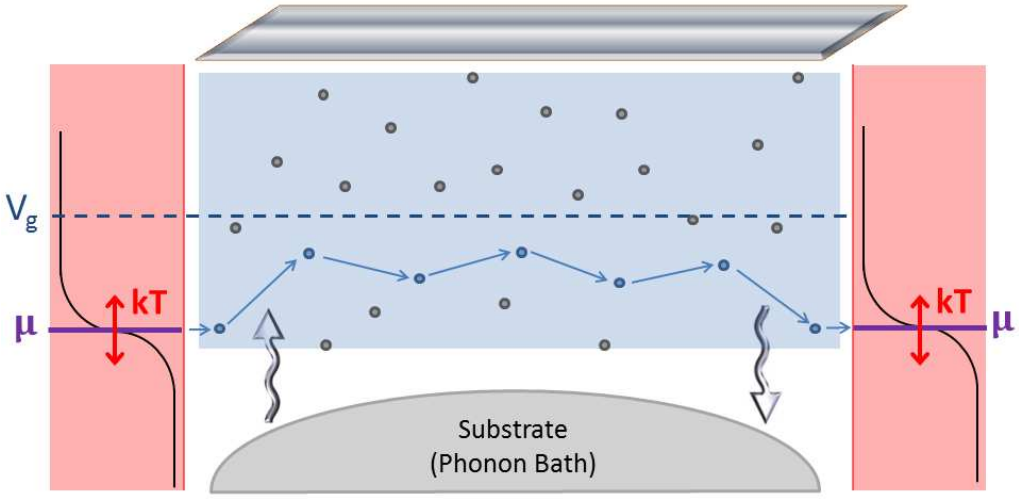

Figure 1. (Color online) Sketch of the device in the field effect transistor configuration. The electronic localized states (blue dots) are located randomly along the nanowire, and their energies are within a band of width E_B (shaded light blue region). A top gate (here in gray) allows to shift the impurity band by a potential V_g which sets its center (dashed line). The left and right electronic reservoirs are characterized by a certain temperature T and electrochemical potential μ at equilibrium. In linear response, electrons in the left reservoir tunnel inside the system in a window of energies of order k_BT around μ. They then move through it via Variable Range Hopping (VRH) before tunneling out on the other side. In doing this, they are thermally assisted by phonons, which allow them to reach states at different energies (wavy lines). The phonons, also at temperature T, are here provided by a substrate.

2. Model and method

We consider a disordered nanowire of length L in which all available electronic states are exponentially localized at positions x_i. We assume each state i is either empty, or occupied by a single electron with a localization length $\xi_i \ll L$, but cannot be doubly occupied owing to a strong on-site Coulomb repulsion[27]. The energy levels E_i of the localized states are distributed within a band of width $2E_B$ and $\nu(E)$ denotes their density of states (DOS) per unit length at energy E. They can be shifted as a whole by an external gate voltage V_g. The nanowire is attached at its ends to two electronic reservoirs held at electrochemical potentials μ_L and μ_R. It is also coupled to a phonon bath which provides the energy for electrons to hop between localized states. We focus on the situation in which the temperature T is the same in all reservoirs and consider linear response, assuming the difference in electrochemical potentials between left and right leads to be small ($\mu_L = \mu + \delta\mu \gtrsim \mu_R \equiv \mu$). The system is sketched in Fig. 1.

2.1. Identification of the different transport mechanisms and of their temperature scales

Transport through the nanowire happens as follows. Since there is a continuum of available states in the leads, we assume that charge carriers, let us say electrons, enter or leave the nanowire

by elastic tunneling processes, without absorbing or emitting phonons §. Inside the nanowire they have the possibility to hop either to states at higher energies by absorbing phonons, or to states at lower energies by emitting them. Determining precisely the favoured electronic paths is a complicated task. The proper way to tackle this issue is to map the hopping model to an equivalent random resistor network [28] and then to reduce it to a percolation problem [27]. Such technical approaches are needed for giving precise quantitative predictions, but at a first stage of analysis, Mott's original argument [29, 30] is actually enough to capture the main features of electronic transport through the nanowire. The key point is that electron transfer from one site to another results from a competition between the elastic tunneling mechanism (controlled by the overlap of the electronic wavefunctions) and the phonon-assisted activated process (controlled by the Boltzmann and Bose factor). Short hops are favoured by the former but are too energy-greedy for the latter, since localized states close in space are far in energy. Mott [29, 30] showed that the optimal electron hopping length is given in one dimension (1D) by $L_M \simeq (\xi/2\nu T)^{1/2}$, assuming the localization lengths and the DOS to be constant in the energy window Δ around μ explored by the electrons ($\xi_i \approx \xi$, $\nu(E) \approx \nu$). Mott's hopping length L_M is a decreasing function of the temperature. One can associate to it two temperature scales : the *activation temperature* $T_x \simeq \xi/(2\nu L^2)$ at which $L_M \simeq L$ and the *Mott temperature* $T_M \simeq 2/(\nu\xi)$ at which $L_M \simeq \xi$. The regime of intermediate temperature $T_x < T < T_M$ is known as the variable-range hopping (VRH) regime. As shown in Fig. 1, electronic transport in this regime is achieved via several jumps of length L_M (with $\xi < L_M < L$). Incidentally (it will be of prime importance later on) the hopping energy Δ, *i.e.* the range of all states around μ which effectively contribute to transport, is given by $\Delta(T) = k_B\sqrt{T_M T}$ from alternative descriptions based on percolation arguments [27, 19, 20]. At lower temperatures $T < T_x$, L_M exceeds the system size and transport through the nanowire is dominated by elastic tunneling processes. On the contrary, at large temperatures $T > T_M$, L_M is found of the order or even smaller than the localization length ξ. This means one enters the nearest-neighbour hopping regime where transport is simply activated between neighbouring localized states. Actually, in 1D, the crossover from VRH to activated transport is expected to take place at temperatures lower than T_M. The reason is the presence of highly resistive regions in energy-position space, where electrons cannot find empty states at distances $\sim \Delta, L_M$. These regions can be circumvented in 2D or 3D but not in 1D,where they behave as "breaks" in the percolating path: electrons are topologically constraint to cross them by thermal activation, making the temperature dependence of the overall resistance simply activated [31, 32]. The critical temperature T_a that marks the onset of this activated behaviour is given implicitely by the relation [33] $L = (\xi/2)(T_M/2T)^{1/2}\exp\{T_M/2T\}$. Below T_a, the probability of having such breaks in the nanowire is negligible.

In Fig. 2 we show how the temperature scales T_x, T_M and T_a are modified when the gate voltage V_g is varied but μ is kept fixed in the reservoirs. The curves have been obtained using the formulas given above, still assuming $\xi_i \approx \xi$ and $\nu(E) \approx \nu$ in the energy range Δ around μ, but taking into account the fact that new electronic states — characterized by an other set of parameters ξ and ν — are involved when the impurity band is shifted with V_g. To plot the curves we used the energy profiles of $\xi(E)$ and $\nu(E)$ corresponding to the Anderson model we will introduce in section 2.3. However the precise shape of those profiles are not important for the present discussion. What matters at this stage is the strong decrease of ξ and ν when one impurity band edge is approached. Such a decrease, expected whatever the model considered, results in a large increase of T_M and T_a that must be eventually cut-off. Indeed, when the DOS ν becomes exponentially small (close to the band edges), the reasoning leading to the formulas

§ Phonon absorption and emission in the electrodes could be straightforwardly taken into account. However, since it does not add any new physics, we neglect it for simplicity's sake.

for T_x, T_M and T_a ceases to be true. We estimate this to happen at an energy scale $|\mu - V_g| \approx \bar{\epsilon}$ where the hopping energy $\Delta(T_M) = k_B T_M$ is maximal *i.e.* becomes comparable to the bandwidth $2E_B$. In the following, $\bar{\epsilon}$ is used to estimate the (effective) positions $V_g \pm \bar{\epsilon}$ of the band edges, beyond which the DOS is possibly finite but extremely small. If $|\mu - V_g| \gtrsim \bar{\epsilon}$ (outside the band), we conjecture that the temperature scales T_M and T_a are approximately constant with V_g and given by their values at $\bar{\epsilon}$. Regarding the activation temperature T_x, we expect $k_B T_x \approx |\mu - V_g| - \bar{\epsilon}$ which is precisely the activation energy that electrons need in order to jump inside the band.

As a summary, let us now associate to each region of the temperature diagram established in Fig. 2 the corresponding regime of electronic transport. Standard VRH regime takes place in region (2a), at intermediate temperatures, when μ lies inside the impurity band. According to Mott law in 1D, the average logarithm of the resistance behaves there as $T^{-1/2}$. Nevertheless, we will see in section 3 that this statement has to be qualified in the vicinity of the band edges, due to the energy dependency of ξ and ν neglected in Mott's approach. At higher temperatures, the temperature dependence of the logarithm of the resistance starts to be activated, namely T^{-1}. This is due either to the presence of a very resistive link in the best conducting path that dominates the resistance (region (3a)), or simply to the fact that the thermal energy $k_B T$ is so high that electrons can jump to nearest neighbours, no matter how far in energy they are (region (4a)). On the contrary at lower temperatures, in region (1a), phonon-assisted hopping mechanisms become negligible: transport takes place via coherent tunnelling processes through the localized states of the nanowire. The thermopower in this regime has been studied by some of the authors in Ref. [34]. If now μ lies outside the impurity band, electrons need to absorb energy in order to enter the band. In region (1b), $k_B T$ is too small for that (the only way for electrons to cross the nanowire is then to tunnel directly from one reservoir to the other, which results in a exponentially vanishing conductance). At higher temperatures, in regions (2b), (3b) and (4b), electrons can be thermally activated. Once they have entered the nanowire, they hop from site to site according to the mechanism prevailing in regions (2a), (3a) and (4a) respectively.

2.2. Formulation in terms of a random resistor network

We follow the approach introduced in Refs. [17, 18] for studying thermoelectric transport in the hopping regime. It consists in solving the Miller-Abrahams resistor network [28] made of all possible links connecting the localized states. The effective resistors between the sites in the nanowire and the leads are also included in the network. Usually (and actually, we did not find a reference where this is not the case) the localization lengths ξ_i of the different states are assumed to be all equal ($\xi_i \approx \xi$) when building the random resistor network. Here we shall go beyond this approximation, being interested in probing the edges of the impurity band where a strong variation of the localization length with the energy E_i is expected. The procedure is summarized below.

Let us consider a pair of localized states i and j. Assuming no correlations between their occupation numbers, the (time-averaged) transition rate from state i to state j is given by the Fermi golden rule as [18]

$$\Gamma_{ij} = \gamma_{ij}\, f_i\,(1 - f_j)\,\left[N_{ij} + \theta(E_j - E_i)\right]\,, \tag{1}$$

where f_i is the average occupation number of state i and $N_{ij} = [\exp\{|E_j - E_i|/k_B T\} - 1]^{-1}$ is the phonon Bose distribution at energy $|E_j - E_i|$. The presence of the Heaviside function accounts for the difference between probabilities of phonons absorption and emission [27]. γ_{ij} is the transition rate associated with phonon-assisted hopping from i to j when i is occupied and j is empty. It is essentially given by the matrix element of the on-site electron-phonon interaction times an overlap

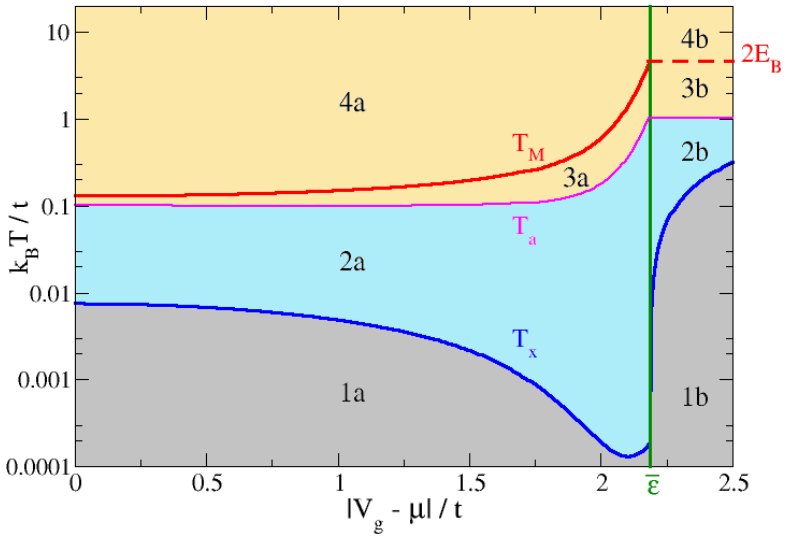

Figure 2. (Color online) Gate dependence of the temperature scales separating the different regimes of electronic transport (elastic regime (gray), VRH regime (blue) and activated regime (red)) in a disordered nanowire. By varying the gate voltage V_g, one scans the impurity band, starting from its center (when $V_g - \mu = 0$) towards its edges (approximately for $|V_g - \mu| = \bar{\epsilon}$) and ending up eventually outside the band (when $|V_g - \mu| \gtrsim \bar{\epsilon}$). The scales T_x, T_a and T_M defined in Sec. 2.1 have been plotted for the Anderson model introduced in Sec. 2.3, with $W = t$ and $L = 1000$.

between the i and j states, and it behaves like

$$\gamma_{ij} \simeq \gamma_{ep} \exp(-2x_{ij}/\xi)\,. \tag{2}$$

Here $x_{ij} = |x_i - x_j|$ is the distance between the states, whereas γ_{ep}, containing the electron-phonon matrix element, is a measure of the electron-phonon coupling and depends on the coupling strength, the phonon density of states and other hidden microscopic parameters. Since it is weakly dependent on E_i, E_j and x_{ij} compared to the exponential factors, it is assumed to be constant. We stress that Eq.(2) is the usual form taken for γ_{ij} but it is correct only if the energy dependence of the localization lengths can be neglected ($\xi_i \approx \xi$) and if $x_{ij} \gg \xi$. Under the widely used approximation [27, 35, 36, 19] which consists in assuming additionally all energy differences E_{ij} larger than $k_B T$, Eq. (1) reduces to:

$$\Gamma_{ij} \simeq \gamma_{ep}\, e^{-2x_{ij}/\xi}\, e^{-(|E_i-\mu|+|E_j-\mu|+|E_i-E_j|)/2k_BT}\,. \tag{3}$$

In the following, we will go beyond this standard approximation by considering the expression (1) for Γ_{ij}, and by replacing Eq. (2) with Eq. (B.4) in order to account for the different localization lengths ξ_i.

The tunneling transition rates between each state i and the leads α ($\alpha = L$ or R) are written in a similar way as

$$\Gamma_{i\alpha} = \gamma_{i\alpha}\, f_i\, [1 - f_\alpha(E_i)] \tag{4}$$

where

$$\gamma_{i\alpha} \simeq \gamma_e \exp(-2x_{i\alpha}/\xi_i)\,. \tag{5}$$

In the above equations $f_\alpha(E) = [\exp\{|E-\mu_\alpha|/k_BT\}-1]^{-1}$ is lead α's Fermi-Dirac distribution, $x_{i\alpha}$ denotes the distance of the state i from lead α and γ_e is a rate quantifying the coupling between the localized states and the leads (taken constant for the same reason as γ_{ep}).

Then, the net electric currents flowing between each pair of localized states and between states and leads are obtained by

$$I_{ij} = e\,(\Gamma_{ij} - \Gamma_{ji}) \tag{6a}$$

$$I_{i\alpha} = e\,(\Gamma_{i\alpha} - \Gamma_{\alpha i}) \qquad \alpha = L, R \tag{6b}$$

$e < 0$ being the electron charge. The linear response solution of this random resistor network problem is reviewed in Ref. [18]. Details of the calculation of the charge currents and heat currents are summarized in Appendix A for the Peltier configuration we consider (where the temperature is T everywhere). Once the total particle/charge (I_L^e) and heat (I_L^Q) currents flowing through the system are known, the electrical conductance G, Peltier coefficient Π and thermopower S follow at once

$$G = \frac{I_L^e}{\delta\mu/e}, \tag{7a}$$

$$\Pi = \frac{I_L^Q}{I_L^e}, \tag{7b}$$

$$S = \frac{\Pi}{T} = \frac{1}{T}\,\frac{I_L^Q}{I_L^e}. \tag{7c}$$

In the last equation, the Onsager symmetry relation [37] $\Pi = ST$ has been used for deducing the thermopower.

2.3. Anderson model for the localized states

The set of energies E_i and localization lengths ξ_i are required as input parameters of the random resistor network problem. To generate them we use the Anderson model. The disordered nanowire is modeled as a 1D lattice described by a $N \times N$ tight-binding Hamiltonian, N being the number of nodes in the lattice, which is equal to the system size L, setting the lattice spacing a equal to one. Its Hamiltonian reads

$$\mathcal{H} = -t\sum_{i=1}^{N-1}\left(c_i^\dagger c_{i+1} + \text{h.c.}\right) + \sum_{i=1}^{N}(\epsilon_i + V_g)c_i^\dagger c_i\,, \tag{8}$$

where $c_i^\dagger$ and c_i are the electron creation and annihilation operators on site i and t is the hopping energy. In the following all energies will be expressed in units of t. The disorder potentials ϵ_i are (uncorrelated) random numbers uniformly distributed in the interval $[-W/2, W/2]$. The constant potential V_g is added to take into account the presence of an external metallic gate, allowing to shift the whole nanowire impurity band.

By diagonalizing the Hamiltonian (8), we find the energies E_i of the localized states. They are distributed with the DOS $\nu(E)$ in the interval $[V_g - E_B, V_g + E_B]$, $\pm E_B$ being the band edges of the model at $V_g = 0$. In the limit $L \to \infty$, $E_B = 2t + W/2$. To generate the localization lengths ξ_i, we neglect sample-to-sample fluctuations and assume that ξ_i is given by the typical localization

length $\xi(E_i)$ at energy E_i, characterizing the exponential decay of the average logarithm of the conductance ($\ln G \sim -2L/\xi$). The DOS $\nu(E)$ and localization length $\xi(E)$ are shown in Fig. 3; their energy dependence is analytically known in the large size and small disorder limit, both in the bulk of the band [38] and close to the edges [39] (see also [34] for a summary). Obviously, if μ lies close to the band edges and/or if the available energy window Δ around μ is not small compared to t, there is no reason to neglect the energy dependency of $\nu(E)$ and $\xi(E)$. This explains why we need to go beyond the usual approximation of constant DOS and localization length, when scanning the impurity band with the gate voltage.

Solving the Anderson model gives us the full set of localized states: their energy levels E_i, their localization lengths $\xi_i = \xi(E_i)$ and in principle their positions along the disordered chain. However, to speed up the procedure of building a basis of localized states, we simply assign the levels E_i to random positions x_i between 0 and L along the chain (with a uniform distribution). This approximation is conventional in numerical simulations of VRH transport (see [40, 33, 18] among others) ‖.

For the sake of clarity, let us mention that in the following we will mainly show results obtained taking $W = t$ to be consistent with Fig. 2. For this value, $E_B = 2.5\,t$ but as shown in Fig. 3, the DOS starts to be infinitely small before reaching the exact band edges $V_g \pm 2.5\,t$. We estimate in that case the energy scale $\bar{\epsilon}$ defined in Sec. 2.1 to $\bar{\epsilon} \approx 2.2\,t$, which sets approximately the (effective) positions of the band edges to $V_g \pm 2.2\,t$.

3. Electrical Conductance

3.1. Background

The electrical conductance of one-dimensional conductors in the VRH regime has been much studied in the literature, both experimentally [41, 42, 43, 44, 45] and theoretically [31, 40, 33, 32, 46, 47]. In particular, the validity of Mott law for the typical conductance

$$\ln G(T) \sim -\alpha \sqrt{\frac{T_M}{T}}, \tag{9}$$

with $\alpha \approx 1$, was a subject of controversy for a long time since, strictly speaking, Mott's argument leading to Eq. (9) does not hold in 1D. It was shown that due to the presence of "breaks", the prefactor α is actually also a function of the temperature and system length [33, 32]. Nevertheless, the T- and L-dependency of α turns out to be so weak that at low temperatures α is almost constant and Mott's law is recovered. Taking the proper $\alpha(L,T)$ into account allows an analytical description of the crossover from Mott's law to the activated behaviour, $\ln G(T) \sim T^{-1}$, above T_a (see Section 2.1) but the refinement thus introduced is too small to be clearly evidenced by numerical simulations and even less by experimental measurements.

Another limitation of Mott's standard argument and of subsequent, more elaborate percolation-based ones is the initial assumption of constant DOS and localization length around μ. As long as $\nu(E)$ is slowly varying in the energy window $|E - \mu| < \Delta$ (still keeping ξ constant), Eq. (9) is expected to hold, but it lacks justification in the case of strongly varying DOS. In

‖ By doing this we lose a feature of Anderson's model, namely that states which are close in energy will be distant in space, and as a consequence our model may overestimate the hopping between certain pairs of states. We argue however that this does not play an important role if the size L of the system is sufficiently large, $L \gg \xi(\mu)$. In this case states which are accidentally close both in space and energy will not only be rare but, more importantly, can merely be seen – regarding percolation – as one small localized cluster, i.e. as a *s*ingle new effective localized state. The reason is that the optimal percolation path is eventually determined by the most resistive links. Thus, we can always reformulate the problem in order to end up in a situation in which neighbouring states are far away in energy.

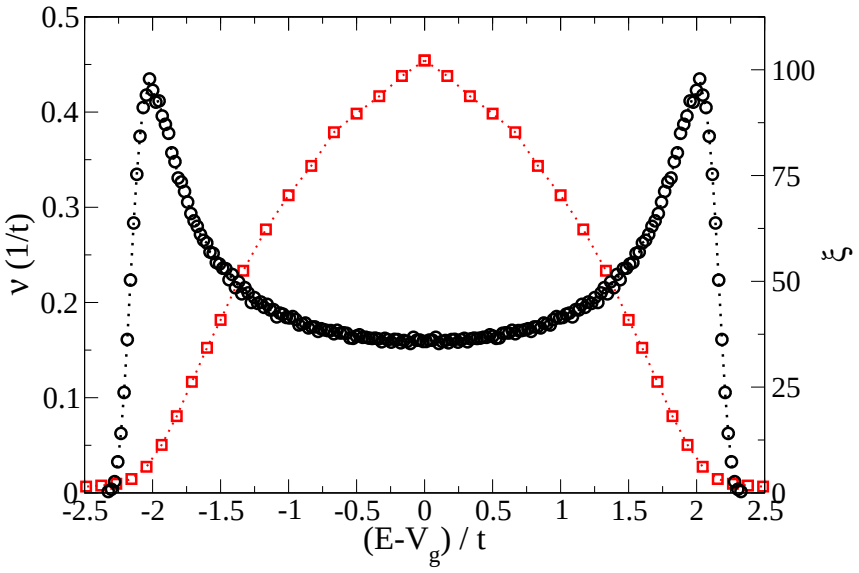

Figure 3. (Color online) Density of states per site ν (○) and localization length ξ (□), as a function of energy E for the 1D Anderson model (8) with disorder amplitude $W/t = 1$. The points correspond to numerical data (obtained in the large length limit with $L = 1600$). Dotted lines are guides to the eye.

particular, Eq. (9) has to be revised when transport through the system occurs at energies around the impurity band edges. This question was tackled by Zvyagin in Refs. [19, 20], by assuming that around the (lowest) band edge ϵ_c, the DOS can be locally approximated by a step-like function of the form

$$\nu(E) \simeq \nu_0\, \theta(E - \epsilon_c). \tag{10}$$

Strictly speaking, he discussed therein hopping conduction in the band tails of *three-dimensional* systems but similar arguments can be applied in 1D. The idea is that when μ lies outside the impurity band, electrons need an activation energy $\epsilon_c - \mu$ in order to "jump" inside it to find available states. This entails an extra term in Eq. (9), which in 1D becomes

$$\ln G(T) \sim -\frac{E_A}{k_B T} - \bar{\alpha}\sqrt{\frac{T_M}{T}}, \tag{11}$$

with $E_A \sim \epsilon_c - \mu$ and $\bar{\alpha}$ differing from α by some numerical factors [48, 20].

3.2. Numerical results

We have investigated numerically how the typical conductance of a disordered nanowire depends on the temperature when the applied gate voltage is varied. For the system described in section 2.3, we have solved the random resistor network problem and calculated the conductance G via Eq.(7a). This procedure has been iterated over many random configurations of the energy levels E_i in order to extrapolate the *typical* logarithm of the conductance $[\ln G]_0$, defined as the median of the resulting distribution $P(\ln G)$¶.

¶ More details concerning the distributions of the logarithm of the conductance for 1D systems in VRH regime are discussed, for instance, in Refs. [33, 49]

In Fig. 4, $[\ln G]_0(T)$ is plotted for two different values of V_g, inside the band and at its very (lowest) edge. In both cases we show that low temperature data exhibits Mott's law $T^{-1/2}$ behaviour (red dashed curve), while at higher temperatures it is well fitted by an activated law of T^{-1}-kind (green dashed curve). A fit to Eq. (11) provides a good interpolation between the two regimes (full blue line). More precisely, when μ lies inside the band (Fig. 4(a)), the validity range of Mott's law ($k_BT/t \lesssim 0.05$) is found to be consistent with the required hypothesis of weakly varying DOS. Indeed, below such temperatures, the energy window $\Delta = k_B\sqrt{T_M T}$ of accessible states around μ is so small ($\Delta \lesssim 0.2$ using for T_M the value given in Fig. 2) that the DOS can be considered as weakly energy dependent ($\Delta\, \partial_E \ln \nu(E)|_\mu \approx 0.3 < 1$). This justifies the validity of Eq. (9) in such a regime. Note that the onset of activated behaviour at $k_BT \approx 0.05\, t$ is also in rough agreement with the predicted value of $k_BT_a \approx 0.1\, t$ in Fig. 2. On the other hand, when μ lies in a region where the DOS is exponentially small (Fig. 4(b)), there is no more reason to use Mott's law to describe our data, even if it appears to be well fitted by Eq. (9) at low temperatures. The point is that other power law formula, $[\ln G]_0 \sim T^\beta$, could be used to fit our data in this narrow temperature range. Thus, one cannot use the apparent suitability of Eq. (9) to support the validity of Mott's law in this regime. Outside the band the correct framework for analysis is provided by Eq. (11). The activated contribution to the conductance is always present, which explains why in Fig. 4(b) the T^{-1} fit starts to be accurate much below the temperature $k_BT_a/t \approx 0.95$. Finally, at very high temperatures (typically larger than t), the typical conductance is found in both cases to decrease with temperature. This is due to the fact that in the limit $T \to \infty$, the factors $f_i(1-f_j)$ and $f_j(1-f_i)$ on one hand, and $f_i(1-f_\alpha)$, $f_\alpha(1-f_i)$ on the other, converge to the same value. Hence, the opposite rates Γ_{ij}, Γ_{ji} and Γ_{iL}, Γ_{Li} tend to level out, which results in a vanishing net current and a divergent resistance. An expansion of the Fermi functions to the next order in inverse temperature yields I_{ij}, $I_{i\alpha} \sim T^{-1}$, which explains the linear decay at high T of $[\ln G]_0$ versus $\ln T$ in Fig. 4 (not emphasized).

4. Thermopower

4.1. Background

The thermopower is a measure of the average energy $\langle E-\mu\rangle$ transferred by charge carriers from the left lead to the right one. In the low temperature coherent regime [34], transport takes place at the Fermi energy. Hence, in linear response with respect to the bias voltage between the two leads, the thermopower is basically determined by the electron-hole asymmetry at μ. On the contrary, in the VRH regime, all states in the energy window $|E-\mu| < \Delta$ are involved. Since $\Delta \gg k_BT$ in this regime, the thermopower benefits from the contribution of states far below and above μ, despite being in linear response. When the gate voltage is adjusted in order to probe the impurity band edges, the electron contribution dominates over the hole one (or vice-versa), yielding an enhanced thermopower.

To study the thermopower in the VRH regime [+], we use the approach introduced by Zvyagin in [19, 20]. The starting point is the percolation theory of hopping transport [19, 20], according to which transport through the system is achieved via percolation in energy-position space. The average $\langle E-\mu\rangle$ is calculated by averaging the energy over the sites composing the percolation

[+] We stress that the usual Mott formula for the thermopower, $S = (\pi^2 k_B^2 T/(3e))\, \partial_E \ln\sigma|_\mu$ (σ being the electrical conductivity), does not apply in the VRH regime, as pointed out by Mott himself in [30]. Indeed, this formula has been derived by averaging $\langle E-\mu\rangle$ within the standard Boltzmann formalism, not suitable in the VRH regime where $\Delta \gg k_BT$.

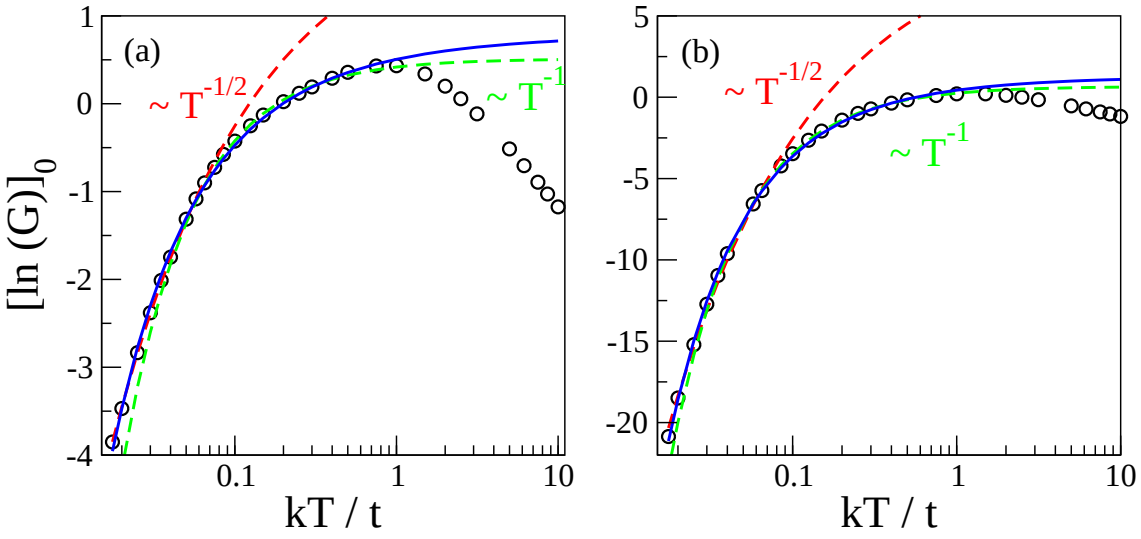

Figure 4. (Color online) Typical value of the logarithm of the conductance $[\ln G]_0$ as a function of temperature for two different values of the gate voltage at $\mu = 0$: (a) $V_g = 1.9\,t$ inside the band and (b) $V_g = 2.3\,t$ at the very edge of the band. In both cases, at low temperatures, numerical data (points) are well fitted by a $T^{-1/2}$ fit (red dashed lines), evolving to a T^{-1} behaviour as T increases (green dashed lines). Full blue lines correspond to Eq.(11), which well interpolates between the two regimes. Parameters: $L = 200$, $W = t$ and $\gamma_e = \gamma_{ep} = t$.

cluster, and the thermopower is given by

$$S = \frac{\langle E-\mu\rangle}{e\,T} = \frac{1}{e\,T}\,\frac{\int dE\,(E-\mu)\,\nu(E)\,p(E)}{\int dE\,\nu(E)\,p(E)}, \tag{12}$$

where $p(E)$ is the probability that a state of energy E belongs to the percolation cluster. The latter quantity is supposed to be proportional to the average number of bonds $N_b(E)$, given by

$$N_b(E) = \int dx \int dE'\,\nu(E')\,\theta\left(\sqrt{\frac{T_M}{T}} - \frac{2x}{\xi} - \frac{|E-\mu| + |E'-\mu| + |E-E'|}{2k_BT}\right), \tag{13}$$

under the assumptions leading to Eq. (3) (low temperature and constant localization length ξ taken at μ, μ assumed inside the band) [27, 20]. The Heaviside function θ accounts for the existence of a percolating path, and restricts the energy range of integration to the window $[\mu-\Delta, \mu+\Delta]$. After integrating over the single spatial variable x (in 1D), one gets

$$p(E) \propto \theta\left(\Delta - |E-\mu|\right) \times \int_{\mu-\Delta}^{\mu+\Delta} dE'\,\nu(E')\left(1 - \frac{|E-\mu| + |E'-\mu| + |E-E'|}{2\Delta}\right)\theta\left(\Delta - |E-E'|\right). \tag{14}$$

Note that if μ lies outside the impurity band, electrons need to jump inside the latter by thermal activation before accessing the percolation cluster. In that case, Equations (13) and (14) have to be modified accordingly, by replacing μ by the energy ϵ_c of the closest band edge and by changing the energy range of integration to $[\epsilon_c, \epsilon_c + \Delta]$ (lower band edge) or $[\epsilon_c - \Delta, \epsilon_c]$ (upper band edge).

Equations (12) and (14) enable us to calculate the thermopower once the DOS $\nu(E)$ is known.

Following Zvyagin's works [19, 20], we discuss below a few extreme cases where the DOS takes a simple form. Contrary to those papers focused on three-dimensional bulk materials, we derive expressions for the thermopower of nanowires in the 1D case. Despite the crudeness of the calculations and the assumptions leading to them, we will see in the next subsection that they are actually enough to qualitatively capture the typical thermopower behaviour and the role of the gate (see Sec. 2).

Let us first consider the case where *(i)* the DOS can be approximated by its first order expansion $\nu(E) \approx \nu(\mu) + (E-\mu)\,\partial_E \ln \nu(E)\big|_\mu$ in the interval $[\mu-\Delta, \mu+\Delta]$, and *(ii)* ν is expected to vary slowly at the scale of Δ, *i.e.* $\Delta\,\partial_E \ln \nu(E)\big|_\mu \ll 1$. Using Eqs. (12) and (14), one finds

$$S \approx \frac{k_B}{e}\left(\frac{k_B T_M}{4}\right)\partial_E \ln \nu(E)\big|_\mu \,. \tag{15}$$

This shows that the thermopower should be temperature independent when the hypothesis above are fulfilled, which is in particular always the case at very low temperatures (bottom part of region (2a) in Fig. 2). Note that the same hypothesis for the DOS lead to the standard Mott formula (9) for the conductance, meaning that Eq. (15) for the thermopower is expected to be valid when the conductance is well described by Eq. (9).

Let us now consider the case where the impurity band edges are explored, say the lower one. In analogy to the previous section, using a rough step-like model for $\nu(E)$ provides useful insight. Substituting an expression of the form (10) in Eq.(12), one gets for the thermopower

$$S = \frac{k_B}{e}\left(\frac{\epsilon_c-\mu}{2k_BT} + \frac{\Delta(T)}{2k_BT}\right) \quad \text{if} \quad \epsilon_c < \mu \quad \text{and} \quad \mu-\epsilon_c < \Delta \tag{16a}$$

$$S = \frac{k_B}{e}\left(\frac{\epsilon_c-\mu}{k_BT} + \frac{\Delta(T)}{2k_BT}\right) \quad \text{if} \quad \epsilon_c > \mu\,, \tag{16b}$$

assuming* $p(E) = 1$ in the energy window $|E-\mu| < \Delta$ $[0 < E-\epsilon_c < \Delta]$ and 0 elsewhere. Similar formulas can be deduced by symmetry if the upper band edge is explored. The resulting thermopower behaviour as a function of temperature turns out to be rich. Indeed, depending on the position of μ with respect to the (bottom) edge ϵ_c of the DOS, and depending on the magnitude of Δ, the thermopower can be an increasing or decreasing function of T. If μ lies outside the impurity band, the thermopower (in unit of k_B/e if not otherwise specified) is found to be a monotonically decreasing function of the temperature (see Eq. (16b)). On the other hand, if μ lies inside the band, close to the edge ϵ_c of the DOS, the thermopower increases with the temperature, reaches a maximum (at $k_BT = (\epsilon_c-\mu)^2/(16k_BT_M)$) and then starts to decrease (see Eq. (16a)).

Let us finally address the large temperature limit ($k_BT \gtrsim 2E_B$), corresponding to region (4b) and the upper part of region (4a) in Fig. 2. In that case, all impurity band states are involved in thermoelectric transport, with $p(E) \approx 1$. As a consequence, the thermopower temperature behaviour is merely $S \sim T^{-1}$. Assuming a constant DOS, one gets

$$S = \frac{k_B}{e}\left(\frac{V_g-\mu}{k_BT}\right). \tag{18}$$

* We have also calculated the thermopower beyond this approximation, by plugging Eq. (10) for $\nu(E)$ into Eq. (14) for $p(E)$. Instead of Eqs. (16a) and (16b), we find respectively

$$S = \frac{k_B}{e}\left[\frac{5(\epsilon_c-\mu)}{8k_BT} + \frac{3\Delta(T)}{8k_BT} + O\left(\frac{\epsilon_c-\mu}{k_BT}\right)\right] \tag{17a}$$

$$S = \frac{k_B}{e}\left[\frac{\epsilon_c-\mu}{k_BT} + \frac{3\Delta(T)}{8k_BT}\right]. \tag{17b}$$

The two sets of equations are obviously very similar. At a qualitative level of analysis, it is meaningless to favour one over the other.

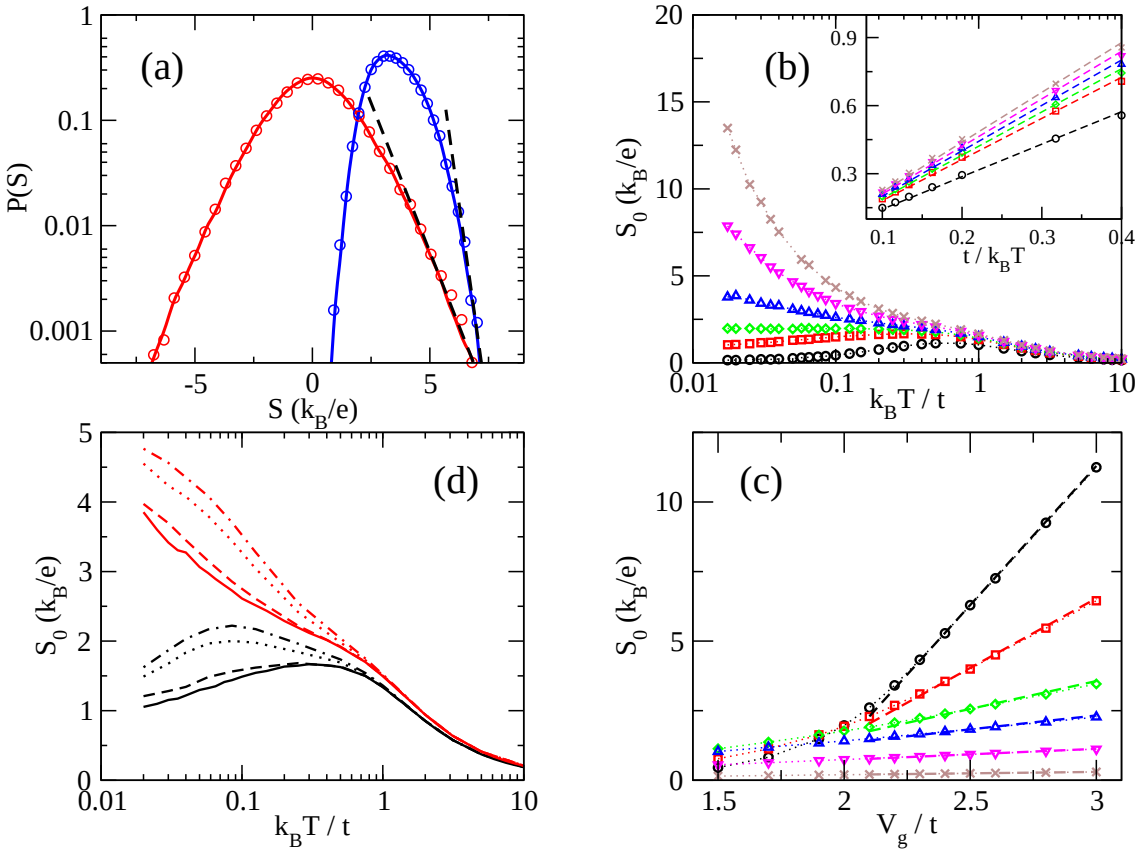

Figure 5. (Color online, in boustrophedon order) In all panels, unless specified, $L = 200$, $\mu = 0$, $W = t$ and $\gamma_e = \gamma_{ep} = t$. (a) Thermopower distributions in the VRH regime, when μ lies in the bulk (left red curve, $V_g = 0$, $W = 4t$) or close to the edge (right blue curve, $V_g = 2.2t$, $W = t$) of the impurity band. Data are given for two lengths of the nanowire ($L = 200$ (full lines) and $L = 400$ (circles)). The straight dashed lines have been drawn to illustrate the exponential behaviour of the tails $\sim \exp\{-cS\}$ [18]. In both cases, $k_BT = t$. (b) Main panel: Temperature dependence of the typical thermopower, around the (lower) band edge. From the bottom to the top, the various curves correspond to $V_g/t = 1.5\,(\circ), 1.9\,(\square), 2.0\,(\diamond), 2.1\,(\triangle), 2.2\,(\triangledown)$ and $2.3\,(\times)$. Dotted lines are guides to the eye. Inset: zoom at very large temperatures $k_BT \gtrsim E_B$. In this situation, the expected $S_0(T)$ is of the form $S_0 \sim T^{-1}$ (see text). Data are plotted versus T^{-1}, dashed lines are linear fits $y = f(V_g)/x$. (c) Typical thermopower as a function of the applied gate voltage, for different values of the temperature ($k_BT/t = 0.1\,(\circ), 0.2\,(\square), 0.5\,(\diamond), 1.0\,(\triangle), 2.5\,(\triangledown)$ and $10.0\,(\times)$). At large V_g (when μ lies outside the band), dashed lines are linear fits with slope t/k_BT (see text). Dotted lines are guides to the eye. (d) Temperature dependence of the typical thermopower, for different values of the electron-phonon coupling ($\gamma_{ep}/t = 1$ (full line), 0.5 (dashed line), 0.1 (dotted line) and 0.05 (mixed line)), at $V_g = 1.9t$ (black curves, bottom set) and $V_g = 2.1t$ (red curves, top set).

4.2. Numerical results

We come back now to the system introduced in Sec. 2.3 and discuss the numerical results obtained for the thermopower by solving the random resistor network (see Appendix A).

We have first studied the thermopower probability distribution $P(S)$ in the VRH regime. Data is shown in Fig. 5(a) for two different gate voltage values, when the impurity band center

(red curve) and lower edge (blue curve) are probed at μ. While the thermopower distribution is symmetric around a vanishing average value at the band center, it is shifted away from 0 and gets skewed close to the band edges. Such features can be easily understood as follows. Let us say a positive V_g is applied in order to probe the lower edge of the impurity band, the level distribution becoming highly asymmetric with respect to μ. Consequently, an electron entering the nanowire from the left lead around μ finds more states to jump to *above* its energy than below. As illustrated in Fig. 1, it has therefore a tendency to absorb energy in order to move to regions of higher DOS, before releasing it at the right side of the nanowire. Recalling that $S = \langle E - \mu \rangle / (eT)$, one can thus explain why $P(S)$ is shifted and skewed at finite V_g. Let us notice that such a skewness is absent in the low-temperature coherent regime [34], where transport only involves electrons at energies very close to μ; in that case, distributions are found to be shifted with V_g but always symmetric. Another important message of Fig. 5(a) is that for both values of V_g the thermopower distribution turns to be independent of the nanowire length L. This is consistent with the recent results published in [18] and the physical picture depicted in Fig. 1, according to which the thermopower in the hopping regime is governed by the edges of the sample.

We have then investigated the typical thermopower behaviour as a function of temperature and gate voltage, by extracting the median S_0 of the distribution $P(S)$ for different sets of parameters. The temperature dependence of S_0 is shown in Fig. 5(b) for different values of the gate voltage, which have been chosen in such a way as to scan the vicinity (in the broad sense) of the lower band edge. Five main features of those curves are worth emphasizing:

(i) S_0 is always positive in unit of k_B/e, hence negative in $\mathrm{V\,K^{-1}}$ (since $e < 0$). The sign of the thermopower reflects the sign of the charge carriers, meaning that here electrons dominate over holes.♯

(ii) At low temperatures the typical thermopower can either increase or decrease with the temperature depending on the gate voltage. Roughly speaking, it increases inside the band and decreases outside, in agreement with the theoretical predictions (16a) and (16b), obtained assuming a step-like model for the DOS close to the band edge ϵ_c. Moreover, the position of the crossover between the two behaviours is found around $V_g - \mu \approx 2t$, a value consistent with our previous estimation of an effective $\epsilon_c \approx V_g - 2.2t$ for the DOS of the Anderson model (see Sec. 2.1).

(iii) At high temperature (typically larger than the bandwidth), the curves converge to a T^{-1} behaviour, as shown in the inset of Fig. 5(b). The crude estimation (18) turns out to be satisfactory in this regime.

(iv) In the low temperature limit and in the case where μ lies inside the band, the typical thermopower S_0 is expected to saturate, according to Eq. (15). Such a saturation is not observed in Fig. 5(b). Two reasons can be invoked. The first one is that Eq. (15) was actually derived under the assumption of a constant localization length $\xi_i \approx \xi(\mu)$ while the numerical results reported here were obtained going beyond this approximation, by taking into account the energy dependency of the different localization lengths ξ_i of sites i. In Appendix B, we show that under the assumption $\xi_i \approx \xi(\mu)$, S_0 indeed saturates at low temperature. The other possibility is simply that the saturation appears at lower temperatures, which are not reachable numerically because of round-off errors.

(v) For high values of V_g, the typical thermopower seems to diverge as the temperature is lowered. It is obvious that the thermopower eventually decreases below a certain temperature, since

♯ We do not exclude however the occurrence of negative S_0 at lower temperature or smaller disorder, even for positive V_g, if the DOS is strongly asymmetric around μ with a negative slope. Besides, this would happen in Fig. 5(b), for some values of V_g, if the energy dependence of ξ was neglected (see Appendix B).

all curves in Fig. 5(b) are known to drop down to zero in the zero-temperature limit (linearly with T and with a positive slope) [34].

In Fig. 5(c), we show how the typical thermopower depends on the gate voltage, for different values of the temperature. Approaching the edge of the impurity band, we see that S_0 increases, the effect being more pronounced at low temperatures. Outside the band, the behaviour of S_0 with V_g is perfectly well fitted by the formula $S_0 = (k_B/e)[\frac{V_g}{k_B T} + f(T)]$, as illustrated by the straight lines in Fig. 5(c). This linear enhancement of S_0 with V_g, as well as its range of validity, is consistent with the prediction (16b) and our initial estimation $\epsilon_c \approx V_g - 2.2t$ for the position of the lower band edge. Note however that Eq. (16b) does not capture the y-intercept $f(T) \approx 0.89 - 1.94/(k_B T)$ of the linear fits. On the other hand the fact that S_0 keeps increasing even outside the impurity band, when the conductance drops exponentially, may seem in contrast with recent experimental observations [5]. We think the explanation lies in the fact that, when the nanowire is almost completely depleted by V_g, the probability for an electron at μ to tunnel inside the band becomes extremely small, and so do the electrical and heat currents; consequently, they may be too hard to measure. Nonetheless their ratio, which gives the thermopower, remains formally well defined and finite.

We conclude our analysis by discussing the order of magnitude of our numerical results. In panels (a), (b) and (c) of Fig. 5, data was obtained taking $\gamma_e = \gamma_{ep} = t$ as input parameters of the model. In panel (d) we investigate how the typical thermopower depends on the choice of these parameters, finding that S_0 does not vary by more than 50% when the ratio γ_e/γ_{ep} is increased or decreased by an order of magnitude. Remarkably, at the lowest studied temperatures (in the VRH regime) and around the band edges, the typical thermopower is found to reach very large values of the order of $10\,(k_B/e) \sim 1\,\mathrm{mV\,K^{-1}}$. It is worthwhile to note that, despite the simplicity of the model, the order of magnitude of these results is comparable to recent measurements of thermopower in semiconducting nanowires [8, 50, 51, 5], showing strong thermoelectric conversion at the band edges.

5. Discussion and conclusion

We have studied thermoelectric transport in a disordered nanowire in the field effect transistor configuration, focusing on intermediate to high temperatures. More precisely, T was high enough for inelastic processes (phonon-assisted hopping between localized states) to be dominant, but still such that $k_B T < 2E_B$, with $2E_B$ the spread in available nanowire states. Transport in this regime is typically of variable range hopping type [29, 30]. We have extended the Miller-Abrahams random resistor network model [28] to deal with band-edge transport, and performed accurate numerical analysis based on the 1D Anderson model. The thermopower shows remarkable gate- and temperature-dependent behaviour, whose features can be understood within a suitable generalization of Zvyagin's analytical treatment of VRH transport [19, 20]. In particular we have showed them to be largely independent of fine system details such as electron-phonon interaction strength or the specific form of the DOS. Our results are in line with numerous experimental observations [8, 50, 51, 5], confirming the great thermoelectric conversion potential of band-edge transport. Notice in particular that semi-quantitative agreement with observations was reached, though we stress that our treatment's strength lies in its general applicability rather than in its high precision – the latter being heavily dependent on fine details of each particular setup, such as materials involved, doping level/type, geometry and so on.

Let us now comment on certain limitations of our treatment. First, interactions have been neglected, except for the requirement of single-occupation of any given localized state [27]. Whereas

this is appropriate in some cases, it is by no means a universally valid assumption. Indeed, numerous delicate issues related to the role of interactions in activated transport are discussed in [36] and references therein. Secondly, we have ignored phonon-drag effects, which is however a much safer bet. It is well known that the latter can play a prominent role in standard band transport – i.e. when electronic states are delocalized – but are irrelevant when transport is due to hopping between localized states[19, 20]. Finally, we have neglected the possibility of the temperature activated transport via delocalized states. This amounts to assuming that $k_BT < E_{del}$, where E_{del} is the distance to the closest region of delocalized states. Clearly E_{del} depends strongly on the system, ranging from tens of Kelvin for weakly doped, crystalline materials, to hundreds of Kelving in amorphous samples [36].

Let us conclude introducing a currently pursued extension of this work. We have seen that a *s*ingle disordered nanowire boasts excellent properties of its *t*ypical thermopower. However the latter exhibits strong sample-to-sample fluctuations, and moreover the nanowire conductance is exponentially small, meaning that no significative power output can reliably be reached. Yet, as mentioned in Sec. 1, stacking numerous wires in parallel could provide a simple and effective workaround to both issues: a array of parallel nanowires is expected to work as an efficient thermoelectric converter (high S) with a conductance scaling roughly linearly with the wire number. Furthermore, an intrinsic asymmetry in the phonon-assisted, band-edge transport problem suggests the possibility of using such an array to generate hot and/or cold spots. Both are issues of paramount technological importance.

Acknowledgments

This work has been supported by CEA through the DSM-Energy Program (project E112-7-Meso-Therm-DSM). We acknowledge stimulating discussions with Y. Imry, R. Jalabert, F. Ladieu, K. Muttalib and A. Parola.

Appendix A. Solution of the random resistor network

In linear response we assume that on each localized state the electron occupation is characterized by a *local distribution* [36, 18]:

$$f_i = f_i^0 + \delta f_i, \tag{A.1}$$

where f_i^0 is the Fermi distribution at equilibrium (i.e., evaluated at the reference values μ and T), and δf_i is the correction induced by the (small) applied bias $\delta\mu$. Linearizing Eqs.(6), and making use of Eqs. (1), (2), and (4), the hopping currents between each pair of localized states, and the tunnelling currents from/to the electrodes can be written in terms of "local potentials" U_i's:

$$\begin{aligned} I_{ij} &= G_{ij}(U_i - U_j), \\ I_{iL(R)} &= G_{iL(R)}(U_i - U_{L(R)}), \end{aligned} \tag{A.2}$$

where

$$\begin{aligned} G_{ij} &= \frac{e^2}{k_BT}\,\gamma_{ij} f_i^0(1-f_j^0)(N_{ij}^0 + 1/2 \mp 1/2), \\ G_{iL(R)} &= \frac{e^2}{k_BT}\,\gamma_{iL(R)} f_i^0(1-f_i^0), \\ U_i &= \frac{k_BT}{e}\,\delta f_i/[f_i^0(1-f_i^0)], \\ U_{L(R)}(\epsilon_i) &= \frac{k_BT}{e}\,\delta f_{L(R)}/[f_i^0(1-f_i^0)]. \end{aligned} \tag{A.3}$$

In the above expressions, in case of double signs, the upper (lower) sign refers to $E_j > E_i$ ($E_j < E_i$). At steady state, according to Kirchoff's conservation law, the net electric current throughout every node i must vanish:

$$\left(\sum_{j\neq i} I_{ij}\right) + I_{iL} + I_{iR} = 0. \tag{A.4}$$

By plugging Eqs. (A.2), we end up with a set of equations (one for every node i) to calculate the U_i's, which can be written conveniently in the matrix form:

$$\sum_j A_{ij} U_j = z_i, \tag{A.5}$$

where

$$\begin{aligned} A_{ij} &= -G_{ij} \qquad (\text{for } i \neq j), \\ A_{ii} &= \sum_{k\neq i} G_{ik} + G_{iL} + G_{iR}, \\ z_i &= G_{iL}\ (\delta\mu_L/e) \end{aligned} \tag{A.6}$$

In writing the expression for z_i, we exploited the fact that $\delta\mu_R = \delta T_R = 0$, having chosen to set the right terminal as reference (see section 2).
Once the system is solved and the U_i are known, all the I_{ij}'s and $I_{iL(R)}$ can be calculated via Eq.(A.2). The overall electric and heat current can be computed by summing the outgoing contributions from the left (or, equivalently, right) lead toward *every* states in the system:

$$\begin{aligned} I^e_L &= -\sum_i I_{iL} = \sum_i I_{iR}, \\ I^Q_{L(R)} &= \sum_i \left(\frac{E_i - \mu_{L(R)}}{e}\right) I_{iL(R)}. \end{aligned} \tag{A.7}$$

Appendix B. Calculation of the hopping probability

Miller and Abrahams[28] described how to calculate the hopping probability γ_{ij} between electronic states localized on donors i and j, mediated by the absorption or emission of a phonon. Their result depends on the (weak) overlap between the electronic wavefunctions in the limit of large distance between the donors, in a way which accounts for the mutual electrostatic effect induced by each of the donors on the other one. It is given by an expression of the kind:

$$\gamma_{ij} \sim \langle\psi_i|\frac{e^2}{\kappa|\boldsymbol{r}-\boldsymbol{r}_i|}|\psi_j\rangle - \langle\psi_i|\psi_j\rangle\langle\psi_i|\frac{e^2}{\kappa|\boldsymbol{r}-\boldsymbol{r}_j|}|\psi_i\rangle. \tag{B.1}$$

If the electronic wavefunctions ψ_i and ψ_j are characterized by the *same* localization length ξ, the above expression leads to a matrix element for a transition $i \to j$ whose main spatial dependence is exponential, given by[28, 36]

$$\gamma_{ij} \sim \exp(-2|\boldsymbol{r}_i - \boldsymbol{r}_j|/\xi). \tag{B.2}$$

This result has been used under less restrictive assumptions by Ambegaokar *et al.*[27].

If the localization lengths of ψ_i and ψ_j are different ($\xi_i \neq \xi_j$), a rigorous evaluation of γ_{ij} may

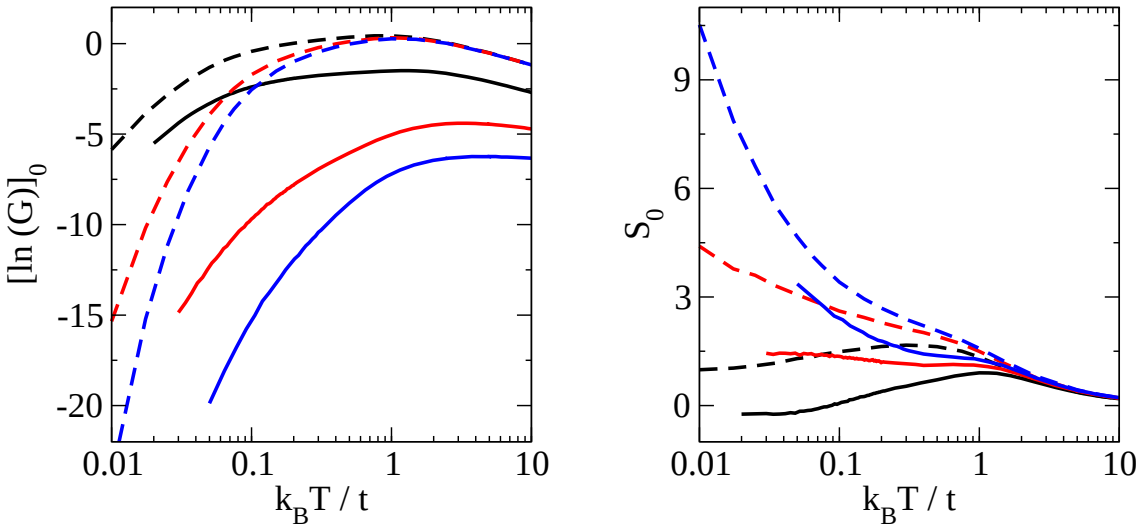

Figure B1. (Color online) Typical logarithm of electrical conductance (left) and typical thermopower (right) of a disordered nanowire as a function of temperature, and for different values of the applied gate voltage. Full lines refer to the case in which all ξ_i are taken equal ($\xi_i = \xi(\mu)$), while dashed lines refer to the case in which the energy dependence of $\xi_i = \xi(E_i)$ in evaluating the transition rate is taken into account. In each set, from the top to the bottom (left) or reversely (right), the various curves correspond to $V_g = 1.9t$ (black), $V_g = 2.1t$ (red) and $V_g = 2.2t$ (blue). Other parameters: $L = 200$, $W = t$, $\mu = 0$, $\gamma_e = \gamma_{ep} = t$.

be complicated, but the key point is that it will always be a function of the overlap $\langle\psi_i|\psi_j\rangle$, and it will be possible to write it in the form

$$\gamma_{ij} \sim \mathcal{A}_{ij} \left|\mathcal{C}_i \exp(-r_{ij}/\xi_i) + \mathcal{C}_j \exp(-r_{ij}/\xi_j)\right|^2 , \tag{B.3}$$

where $r_{ij} = |\boldsymbol{r}_i - \boldsymbol{r}_j|$ is the distance between i and j, and the coefficients $\mathcal{A}_{ij}$, $\mathcal{C}_i$ and $\mathcal{C}_j$ depend on ξ_i, ξ_j and r_{ij}. The explicit form of these coefficients will take into account all the details concerning the wavefunction overlap. In 1D the calculation can be done quite easily and leads to

$$\begin{aligned}\gamma_{ij} =& \mathcal{A}_{ij} \left(\frac{1}{\xi_i} - \frac{1}{\xi_j}\right)^{-2} \left(\frac{\exp\{-2r_{ij}/\xi_j\}}{\xi_i^2} + \frac{\exp\{-2r_{ij}/\xi_i\}}{\xi_j^2}\right. \\ & \left. - \frac{2\exp\{-r_{ij}(1/\xi_i + 1/\xi_j)\}}{\xi_i \xi_j}\right) .\end{aligned} \tag{B.4}$$

This is the expression that we use in modelling our system.

In order to estimate the difference between taking into account or neglecting the energy dependence of $\xi(E)$ when computing the transition rates (Eqs.(1) and (4)), we show here a comparison between the typical logarithm of the conductance and the typical thermopower as functions of the temperature, evaluated in the two cases. Fig. B1 clearly shows that there is no *qualitative* difference between the curves computed using $\xi(\mu)$ (dashed lines) and $\xi(E)$ (full lines). The main effect of taking into account the localization length energy dependence is that, according to Eq.(B.4), all transitions toward the more delocalized states around the band center are favoured. This leads to a much better conductance especially at low temperatures, where the difference could be of several orders of magnitude; on the other hand, the effect on the thermopower is less important.

References

[1] Chen G, Dresselhaus M S, Dresselhaus G, Fleurial J P and Caillat T 2003 *Int. Mater. Rev.* **48** 45
[2] Hicks L D and Dresselhaus M S 1993 *Phys. Rev. B* **47** 16631
[3] Curtin B M, Fang E W and Bowers J E 2012 *J. Electron. Mat.* **41** 887
[4] Blanc C, Rajapbour A, Volz S, Fournier T and Bourgeois O 2013 *Appl. Phys. Lett.* **103** 043109
[5] Brovman Y M, Small J P, Hu Y, Fang Y, Lieber C M and Kim P 2013 *arXiv:1307.0249*
[6] Stranz A, Waag A and Peiner E 2013 *J. Electron. Mat.* **42** 2233
[7] Karg S, Mensch P, Gotsmann B, Schmid H, Kanungo P D, Ghoneim H, Schmidt V, Björk M T, Troncale V and Riel H 2013 *J. Electron. Mat.* **42** 2409
[8] Roddaro S, Ercolani D, Safeen M A, Suomalainen S, Rossella F, Giazotto F, Sorba L and Beltram F 2013 *Nano Lett.* **13** 3638
[9] Hochbaum A I, Chen R, Delgado R D, Liang W, Garnett E C, Najarian M, Majumdar A and Yang P 2008 *Nature* **451** 163
[10] Tilke A, Pescini L, Erbe A, Lorenz H and Blick R H 2002 *Nanotechnology* **13** 491
[11] Bourgeois O, Fournier T and Chaussy J 2007 *J. Appl. Phys.* **101** 016104
[12] Boukai A I, Bunimovich Y, Tahir-Kheli J, Yu J K, Goddard W A and Heath J R 2008 *Nature* **451** 168
[13] Galli G and Donadio D 2010 *Nat. Nanotech.* **5** 701
[14] Heron J S, Bera C, Fournier T, Mingo N and Bourgeois O 2010 *Phys. Rev. B* **82** 155458
[15] He Y and Galli G 2012 *Phys. Rev. Lett.* **108** 215901
[16] Hu M and Poulikakos D 2012 *Nano Lett.* **12** 5487
[17] Jiang J H, Entin-Wohlman O and Imry Y 2012 *Phys. Rev. B* **85** 075412
[18] Jiang J H, Entin-Wohlman O and Imry Y 2013 *Phys. Rev. B* **87** 205420
[19] Zvyagin I P 1973 *Phys. Stat. Sol. (b)* **58** 443
[20] Zvyagin I P 1991 *Hopping Transport in Solids* (ed. by M. Pollak and B. I. Shklovskii (North-Holland, Amsterdam))
[21] Feser J P, Sadhu J S, Azeredo B P, Hsu K H, Ma J, Kim J, Seong M, Fang N X, Li X, Ferreira P M, Sinha S and Cahill D G 2012 *J. Appl. Phys.* **112** 114306
[22] Li Y, Buddharaju K, Singh N and Lee S 2012 *J. Electron. Mat.* **41** 989
[23] Poirier W, Mailly D and Sanquer M 1993 *Phys. Rev. B* **59** 10856
[24] Tilke A, Blick R H, Lorenz H, Kotthaus J P and Wharam D A 1999 *Appl. Phys. Lett.* **75** 3704
[25] Dayen J F, Wader T L, Rizza G, Golubev D S, Cojocaru C S, Pribat D, Jehl X, Sanquer M and Wegrowe J E 2009 *Eur. Phys. J. Appl. Phys.* **48** 10604
[26] Rodin A S and Fogler M M 2010 *Phys. Rev. Lett.* **105** 106801
[27] Ambegaokar V, Halperin B I and Langer J S 1971 *Phys. Rev. B* **4** 2612
[28] Miller A and Abrahams E 1960 *Phys. Rev.* **120** 745
[29] Mott N F 1969 *Phil. Mag.* **19** 835
[30] Mott N F and Davis E A 1979 *Electronic Processes in Non Crystalline Materials* (Clarendon, Oxford, (2nd ed.))
[31] Kurkijärvi J 1973 *Phys. Rev. B* **8** 922
[32] Raikh M E and Ruzin I M 1989 *Sov. Phys. JETP* **68** 642
[33] Serota R A, Kalia R K and Lee P A 1986 *Phys. Rev. B* **33** 8441
[34] Bosisio R, Fleury G and Pichard J L 2014 *New J. Phys.* **16** 035004
[35] Pollack M 1972 *J. Non-Cryst. Solids* **11** 1
[36] Shklovskii B and Efros A 1984 *Electronic Properties of Doped Semiconductors* (Springer-Verlag, Berlin)
[37] Callen H 1985 *Thermodynamics and an Introduction to Thermostatics* (John Wiley and Sons, New York)
[38] Kramer B and MacKinnon A 1993 *Rep. Prog. Phys.* **56** 1469
[39] Derrida B and Gardner E 1984 *J. Physique* **45** 1283
[40] Lee P A 1984 *Phys. Rev. Lett.* **53** 2042
[41] Kwasnick R F, Kastner M A, Melngailis J and Lee P A 1984 *Phys. Rev. Lett.* **52** 224
[42] Webb R A, Hartstein A, Wainer J J and Fowler A B 1985 *Phys. Rev. Lett.* **54** 1577
[43] Ladieu F, Mailly D and Sanquer M 1993 *J. Phys. I France* **3** 2321
[44] Hasko D G, Cleaver J R A, Ahmed H, Smith C G and Dixon J E 1993 *Appl. Phys. Lett.* **62** 2533
[45] Han M Y, Brant J C and Kim P 2010 *Phys. Rev. Lett.* **52** 224
[46] Ladieu F and Bouchaud J P 1993 *J. Phys. I France* **3** 2311
[47] Rodin A S and Fogler M M 2011 *Phys. Rev. B* **84** 125447
[48] Grant A J and Davis E A 1974 *Sol. State Comm.* **15** 563
[49] Rodin A S and Fogler M M 2009 *Phys. Rev. B* **80** 155435
[50] Moon J, Kim J H, Chen Z, Xiang J and Chen R 2013 *Nano Lett.* **13** 1196
[51] Tian Y, Sakr M R, Kinder J M, Liang D, MacDonald M J, Qiu R L J, Gao H J and Gao X P A 2012 *Nano Lett.* **12** 6492